

Perturbative predictions for B_c meson production in hadronic collisions

Marco Masetti

Dipartimento di Fisica, Università di Roma “Tor Vergata”,
and I.N.F.N., Sezione di Roma II, Viale della Ricerca Scientifica
I-00133 Roma, Italy

Francesca Sartogo

Dipartimento di Fisica, Università di Roma “la Sapienza”,
and I.N.F.N., Sezione di Roma, Piazzale A. Moro 2,
I-00185 Roma, Italy

March 31, 1995

Abstract

Perturbative cross section for direct B_c meson production in gluon gluon scattering $gg \rightarrow B_c^+ b\bar{c}$ is calculated and compared with other existing results. Predictions for hadronic B_c production at Tevatron and LHC are presented and the main sources of uncertainties are discussed.

In the last years many theoretical studies on B_c meson properties were published, but an experimental identification of this pseudoscalar bound state formed by two quarks with different flavours is still missing, due to the very small production cross section.

The mass spectrum of $\bar{b}c$ bound states is expected to be similar to the spectra of other mesons with two heavy quarks (charmonium and bottomonium) and predictions based on potential models and on QCD sum rules [1, 2] indicate the presence of a rich structure of excited states below the fragmentation threshold in a B and a D meson. There is however an important difference with respect to unflavoured quarkonia: the excited states cannot decay directly into light mesons, but decay only to the pseudoscalar B_c ground state, due to the flavour conservation in strong and electromagnetic interactions. The lifetime of the weak-decaying B_c meson is expected to be in the range of D mesons lifetimes [3, 4]. Exclusive B_c decays were studied by several authors [3, 4, 5]. Some decay modes are interesting for experimental detection, for example the semileptonic decay with three charged leptons in the final state ($B_c \rightarrow J/\psi + l + \nu_l$ followed by the electromagnetic decay $J/\psi \rightarrow l'^+ + l'^-$) with composite branching ratio of about 10^{-2} , and the decay in $J/\psi + \pi$, with branching ratio of the order of 10^{-3} . The lack of experimental detection of B_c mesons is a consequence of the small production cross section: in fact the production via electromagnetic or strong interaction requires two additional heavy quarks in the final state, and is therefore suppressed at typical experimental energies. The production of a B_c without other heavy particles should be possible in processes like $e + \nu \rightarrow W^* \rightarrow B_c$, which however involve weak interactions and are strongly suppressed due to the high virtuality of the W^* .

The standard estimates of B_c production cross section are based on perturbative calculations with the heavy quark bound state described in the zero binding energy limit. The simplest but important case of B_c production in $e^+ e^-$ annihilation involves only four Feynman diagrams and was studied in detail [6]. The total branching ratio for Z^0 with a B_c^+ or a B_c^- in the final state (including the contribution due to the production of excited B_c states which subsequently decay to the ground state) is predicted to be $140 \cdot 10^{-6}$ i. e. $\sigma(Z^0 \rightarrow B_c^\pm X) \sim 10^{-3} \sigma(Z^0 \rightarrow b \bar{b} X)$. An estimate obtained with the Montecarlo event generator Herwig, which for Z^0 decays in B_c^\pm gives similar results, indicates that also at high energy hadronic colliders like Tevatron and LHC the B_c^\pm production cross section would be around 10^{-3} times the $b\bar{b}$ production cross section [7].

In the perturbative approach the relevant process for B_c hadroproduction is the gluon gluon scattering $g g \rightarrow B_c^+ b \bar{c}$, which at the lowest order involves 36 diagrams. The process $q\bar{q} \rightarrow B_c^+ b \bar{c}$ is expected to give a negligible contribution to the hadronic B_c production cross section. The calculation is extremely simplified if one considers only the *fragmentation* terms [8], which were expected to dominate at high energy; however this approach fails at least in the photoproduction process, as shown in [9]. The complete perturbative calculation for $g g \rightarrow B_c^+ b \bar{c}$ was performed by several authors [11, 12, 13], with results in disagreement with each other.

From this summary of theoretical predictions about the B_c mesons it should be clear that high energy hadronic colliders give the best chances to identify these particles, and it is therefore necessary to reduce the large uncertainties due to the discrepancies between

existing predictions. For this reason in this letter we present the results of an independent study on direct B_c hadroproduction. The dependence of the results on different choices of the gluon distribution functions and on the scale for α_s , which are the main sources of uncertainty, is discussed. Our results are definitely incompatible with [11] and [13], which however give predictions differing with each other at least by a factor 20, difficult to ascribe only to different choices of gluon distribution functions. On the other hand our results are essentially in agreement with [12].

The calculation technique is standard: in the approximation of negligible binding energy and relative momentum in the bound state, which is justified for bound states with only heavy constituents, the quarks are on shell and have parallel momenta ($m_b p_c^\mu = m_c p_b^\mu$) and the meson mass is $M_{B_c} = m_c + m_b$. The 36 Feynman diagrams for the process $g g \rightarrow B_c^+ b \bar{c}$ can be obtained from the 13 diagrams of fig. 1 performing all possible interchanges of initial gluon momenta and of final quark flavours. The rule to describe the bound state in this approximation is to insert as ‘bound state vertex’ the spin projector

$$\frac{\delta^{cc'}}{\sqrt{N_c}} \frac{f_{B_c}}{\sqrt{48}} \Gamma (\not{p} + M_{B_c})$$

where c and c' are colour indices and $\Gamma = \gamma_5$ for a pseudoscalar meson while $\Gamma = \not{\epsilon}$ for a vector meson. The decay constant f_{B_c} is defined by

$$< 0 | \bar{b} \gamma_\mu \gamma_5 c | B_c(P) > = i f_{B_c} P_\mu$$

and in the non relativistic limit it is proportional to the wave function in the origin:

$$f_{B_c} = \sqrt{\frac{12}{M_{B_c}}} |\Psi(0)|.$$

The simple substitution of the sum on external gluon polarizations $\sum_{i=1,2} \varepsilon_{i\mu} \varepsilon_{i\nu}$ with $g_{\mu\nu}$ would give ghost contributions. It is possible to avoid ghosts summing only on physical transversal polarizations:

$$\sum_{i=1,2} \varepsilon_{i\mu} \varepsilon_{i\nu} = -g_{\mu\nu} + \frac{k_\mu n_\nu + k_\nu n_\mu}{k \cdot n} - \frac{k_\mu k_\nu}{(k \cdot n)^2}$$

where k is the gluon momentum and we choose $n^\mu = (k_a^\mu + k_b^\mu)/\sqrt{\hat{s}}$. The number of independent terms in the cross section can be greatly reduced using relations between amplitudes connected by exchange of the initial gluons or of final quarks flavours and momenta. Using the algebraic program Schoonschip [14] we calculate the squared amplitude and integrate analytically to obtain the differential partonic cross section $d^2 \hat{\sigma} / dp_T dy$, where p_T is the transverse momentum and y is the c.m. rapidity of the produced B_c . The subsequent integrations are performed both using the Montecarlo integration program Vegas [15] and using simple algorithms for numerical evaluation of low dimensional integral, to check the convergence of the result.

$\sqrt{\hat{s}}(\text{GeV})$	$\hat{\sigma}$	$\hat{\sigma}$ [11]	$\hat{\sigma}$ [12]
20	23.6	5.3	22.5
30	26.0	9.2	—
40	22.3	—	30.8
60	15.5	8.6	—
80	11.2	—	—
100	8.4	—	16.2

Table 1: Cross section (in pb) for $g g \rightarrow B_c^+ b \bar{c}$. All the results are rescaled to $f_{B_c} = 500$ MeV.

As a preliminary step and a check of our calculation we studied the direct production in photon photon collisions $\gamma \gamma \rightarrow B_c^+ b \bar{c}$. At the lowest order of perturbation theory this process involves 20 diagrams which can be obtained from those of fig. 1 eliminating the diagrams containing non abelian vertices, and replacing the external gluons with photons. This calculation was already performed in [9] and [10]. Our results for this process, using the same values for the parameters m_b , m_c , f_{B_c} , α_s , α_{em} , are in good agreement with those of [9] and [10].

For the process $g g \rightarrow B_c^+ b \bar{c}$ we use the following values of the parameters:

$$f_{B_c} = 500 \text{ MeV}, \quad \alpha_s = 0.2, \quad M_{B_c} = 6.3 \text{ GeV}, \quad m_b/m_c = 3$$

Note that the partonic cross section is a function of the kinematical variables times $f_{B_c}^2 \alpha_s^4$, and therefore the rescaling of the results for different values of f_{B_c} and α_s is easy to obtain.

The total cross section for this process as a function of the energy in the partonic center of mass $\sqrt{\hat{s}}$ is plotted in fig. 2, while the differential partonic cross sections $d\hat{\sigma}/dp_T$ and $d\hat{\sigma}/dy$ are shown for different values of \hat{s} in fig. 3 and fig. 4.

In Tab. 1 the total partonic cross section for several values of \hat{s} is compared with the analogous existing calculations [11, 12], rescaling all the results to the same value of f_{B_c} . Unfortunately the comparison is made difficult by the small amount of information on the partonic cross section before the convolution with the gluon distribution functions. The results of [11] are significantly smaller than ours. Even if it is not clear to us if their results refer to a fixed value of α_s or a running one, and in this last case which scale they choose, the difference cannot be explained simply by the running of α_s .

In [12] α_s is fixed to 0.2 and $f_{B_c} = 570$ MeV; with the appropriate rescaling of f_{B_c} our results are in reasonable agreement with theirs in the low \hat{s} region. Given the behaviour of the partonic cross section, the discrepancies between the values we obtain and those obtained by [12] at higher energies are not really relevant in the evaluation of the hadronic cross section, after the convolution with the gluon distribution functions. Finally, a comparison with [13] is impossible at this level, since only results on the hadronic cross section are discussed there.

$\sqrt{s}(\text{TeV})$		gluon distribution	scale	σ (nb)	σ (nb) <i>this paper</i>
0.12	[11]	EHLQ	$\hat{s}/4$	$4.5 \cdot 10^{-3}$	$60. \cdot 10^{-3}$
1.8				1.0	8.5
16.				12.3	78
1.8	[12]	[12]	\hat{s}^*	9.4	8.8
16.			\hat{s}^*	151	140
1.8	[13]	CTEQ	\hat{s}	18.3	2.5
1.8			$\hat{s}/4$	29.6	3.8
1.8			$4M_{B_c}^2$	31.5	3.9

Table 2: Comparison of hadronic cross section (in nb). All results are rescaled to $f_{B_c} = 500$ MeV. In the fourth column we indicate the scale for gluon distribution functions and running α_s ; the * indicates results obtained for fixed $\alpha_s = 0.2$, evolving only the gluon distribution. In the fifth and sixth column the cross sections obtained in the cited papers and the values we obtain using the same prescriptions are reported.

The cross section for the hadronic processes $p p \rightarrow B_c^+ X$ and $p \bar{p} \rightarrow B_c^+ X$ can be obtained by the convolution of the partonic cross section with the gluon distribution functions $g(x, Q^2)$:

$$\sigma(s) = \int_0^1 dx_1 \int_0^1 dx_2 g(x_1, Q^2) g(x_2, Q^2) \theta(x_1 x_2 s - 4M_{B_c}^2) \hat{\sigma}(\hat{s} = x_1 x_2 s).$$

In figs. 5 and 6 the differential cross section in p_T and y_{lab} obtained with the MRS(A) gluon distribution function [16] is plotted for the energies corresponding to Tevatron (1.8 TeV) and LHC (14 TeV).

In Tab. 2 we compare the values for direct B_c^+ production cross section in proton proton collisions reported in [11, 12, 13], with the results we obtain using the same prescriptions and gluon distribution functions (EHLQ [18], CTEQ [19] and the parametrization described in [12]). In [11] the EHLQ gluon distribution function is used fixing the evolution scale Q^2 at $\hat{s}/4$. With the same gluon distribution and the same Q^2 we obtain for the hadronic cross section values greater of those of [11] especially at the lower energies. This comparison confirms the disagreement with [11] already observed for the partonic cross section.

To compare our predictions with [12], we fix $\alpha_s = 0.2$ as they do, and we use the same parametrization of gluon distribution function they describe in [12] with an evolution scale $Q^2 = \hat{s}$. There is agreement between our results and those of [12], especially at the lower energy. The results of [13] are much larger than all other existing predictions. We obtain results which are smaller than those of [13] by at least a factor 7, using the same gluon distribution (CTEQ) and the same evolution scale as they do, and therefore we

gluon distribution	Q^2	σ (nb) $\sqrt{s} = 1.8$ TeV	σ_0 (nb) $\sqrt{s} = 1.8$ TeV	σ (nb) $\sqrt{s} = 14$ TeV	σ_0 (nb) $\sqrt{s} = 14$ TeV
MRS(A)	\hat{s}	3.2	7.3	44	110
MRS(A)	$4M_{B_c}^2$	4.9	6.6	61	80
MRS(G)	\hat{s}	3.3	7.4	57	139
MRS(G)	$4M_{B_c}^2$	5.2	6.9	82	109
GRV	\hat{s}	3.9	8.8	81	196
GRV	$4M_{B_c}^2$	6.4	8.6	121	163
[12]	\hat{s}	3.8	8.8	47	121
[12]	$4M_{B_c}^2$	5.8	7.8	62	84
EHLQ	\hat{s}	5.6	9.4	60	113
EHLQ	$4M_{B_c}^2$	8.8	8.1	77	71

Table 3: Hadronic cross section (in nb) with $f_{B_c} = 500$ MeV; Q^2 is the scale for gluon distribution functions; σ and σ_0 are the cross sections calculated with running $\alpha_s(Q^2)$ and with fixed $\alpha_s = 0.2$ respectively. We put in evidence the maximum and minimum value obtained for running $\alpha_s(Q^2)$ using the more updated gluon distribution parametrizations.

conclude that the incompatibility of our results with those of [13] is not related to the choice of gluon distribution functions and can be only a consequence of a disagreement in the calculation of the partonic cross section $\sigma(g g \rightarrow B_c^+ b \bar{c})$.

In Tab. 3 the results we obtain with several gluon distribution functions (MRS(A) and MRS(G) [16], GRV [17], EHLQ [18], and the parametrization of [12]) are shown. While the choice of the gluon distribution function parametrization EHLQ and [12] is mainly dictated by the comparison with other existing results, it is also interesting to show the values obtained with other updated sets of gluon distribution functions. In order to discuss the possible dependence of the results on the evolution scales for the gluon distributions and for the running coupling constant α_s , we vary Q^2 between $4M_{B_c}^2$ and \hat{s} . The case of fixed α_s ($\alpha_s = 0.2$) is also considered, as suggested in [12]. We will not attempt to justify a particular choice of the evolution scale in the leading order calculation described here; it is however clear that results obtained fixing $\alpha_s = 0.2$ must be considered as optimistic higher limits on the predicted cross sections. It should be noted that the relatively high result one obtains using EHLQ and α_s running is due to the relatively high value of Λ_{QCD} rather than to the shape of the gluon distribution function. The difference in the choice of the gluon distribution function however emerges more clearly at the energy corresponding to LHC. While at the energy of Tevatron the relevant x region is $x \gtrsim 10^{-4}$, in the case of LHC it becomes $x \gtrsim 10^{-6}$. All gluon distribution parametrizations are expected to be valid only above a given x_{min} (a typical value is $x_{min} = 10^{-5}$) and therefore the cross sections at higher energies are typically underestimated. The only exception is the GRV gluon distribution function, for which $x_{min} = 10^{-6}$, but it has to be noted that the shape

of the GRV gluon is considerably steeper than, for example, the MRS(G) gluon, which comes from a recent analysis of the latest measurements of the structure function F_2 at HERA [16]. The predicted cross section for direct B_c production at Tevatron and LHC, taking into account the uncertainties on the knowledge of the behaviour of the gluon at very small x , can be obtained with MRS and GRV gluon distributions:

$$\sigma_{direct}(p\bar{p} \rightarrow B_c^+ X) = \frac{f_{B_c}^2}{(500 \text{ MeV})^2} (3.2 - 6.4) \text{ nb} \quad (\text{Tevatron; } 1800 \text{ GeV});$$

$$\sigma_{direct}(pp \rightarrow B_c^+ X) = \frac{f_{B_c}^2}{(500 \text{ MeV})^2} (0.04 - 0.12) \mu\text{b} \quad (\text{LHC; } 14 \text{ TeV}).$$

A possible important source of uncertainty in the predicted cross sections is the factor $f_{B_c}^2$. The existing predictions vary from $f_{B_c} = 160 \text{ MeV}$ [20] to $f_{B_c} = 600 \text{ MeV}$ [21]. Varying f_{B_c} between so different values would give a contribution to the uncertainty much larger than those due to the choices of parton distributions and of evolution scales. A more careful inspection of the predictions shows that potential models have a much smaller uncertainty ($f_{B_c} = 500 \pm 80 \text{ MeV}$: for a detailed discussion and review of predictions for f_{B_c} see [2]), while QCD sum rules give results spread in a wide interval, due to the intrinsic ambiguities of the method. However in [2] it is asserted that the most reliable predictions from QCD sum rules are compatible with potential models ($f_{B_c} = 460 \pm 60 \text{ MeV}$). The simpler way to obtain predictions for f_{B_c} and for the $c\bar{b}$ spectrum is to rescale the charmonium and bottomonium spectra to the intermediate case of $c\bar{b}$ bound states: this is the role of potential models which can be considered as a sort of parametrization of quarkonium spectra which gives predictions for B_c . For this reason it seems to us that potential models are presently more reliable than QCD sum rules for phenomenological predictions on $c\bar{b}$ spectrum and wave functions. Considering only potential model predictions, the uncertainty in B_c production cross sections due to the factor $f_{B_c}^2$ is about 30%, much smaller than the uncertainty from α_s and gluon distributions.

Finally we want to give an estimate of the total B_c production cross section in hadronic collisions, including the contribution due to the production of excited $c\bar{b}$ states which subsequently decay to pseudoscalar B_c . The main contribution should come from vector B_c^* production. In [12] this cross section is calculated obtaining $\sigma(pp \rightarrow B_c^* X) \simeq 2.5\sigma(pp \rightarrow B_c X)$. Neglecting further contributions from other excited B_c states we conclude that the total cross section for the production of B_c^+ and B_c^- would be

$$\sigma_{total}(p\bar{p} \rightarrow B_c^+ X) \sim 20 - 50 \text{ nb} \quad (\text{Tevatron; } 1800 \text{ GeV});$$

$$\sigma_{total}(pp \rightarrow B_c^+ X) \sim 0.3 - 0.8 \mu\text{b} \quad (\text{LHC; } 14 \text{ TeV}).$$

This correspond to at least one thousandth of the total $b\bar{b}$ production cross section.

In this letter we discussed the main sources of uncertainties in the calculation of the cross section for direct B_c meson production in hadronic collisions at the lowest order of perturbation theory and in the zero binding energy limit. The uncertainties related to the choice of input parameters and of gluon distribution parametrizations amount roughly to a factor 3, too small to explain the large discrepancies between the different existing calculations. Finally we gave an estimate of the total B_c production cross section, including the contribution of excited states, for Tevatron and LHC.

We thank M. Lusignoli for having drawn our attention to the problem treated in this letter and for many useful discussions and comments. We are also grateful to A. K. Likhoded, V. Lubicz, S. Petrarca and B. Taglienti.

References

- [1] E. Eichten et al., Phys. Rev. D17 (1979) 3090; E. Eichten et al., Phys. Rev. D21 (1980) 203; S. Godfrey, N. Isgur, Phys. Rev. D32 (1985) 189; S. S. Gershtein et al., Int. J. Mod. Phys. A6 (13) (1991) 2309; E. Eichten, C. Quigg, Phys. Rev. D49 (1994) 5845.
- [2] V. V. Kisilev, A. K. Likhoded, A. V. Tkabaladze, preprint hep-ph 9406339.
- [3] M. Lusignoli, M. Masetti, Z. Phys. C51 (1991) 549.
- [4] P. Colangelo, G. Nardulli, N. Paver, Z. Phys. C57 (1993) 43.
- [5] E. Jenkins et al., Nucl. Phys. B390 (1993) 463; V. V. Kisilev, A. V. Tkabaladze, Phys. Rev. D48 (1993) 5208; E. Bagan, preprint CERN-TH7141/94 hep-ph9403208; M. Masetti, Phys. Lett. B 286 (1992) 160.
- [6] L. Clavelli, Phys. Rev. D26 (1982) 1610; C. R. Ji, F. Amiri, Phys. Rev. D35 (1987) 3318; F. Amiri, C. R. Ji, Phys. Lett. B195 (1987) 593; V. Barger, K. Cheung, W. Y. Keung, Phys. Rev. D41 (1990) 1541; C. H. Chang, Y. Q. Chen, Phys. Lett. B284 (1992) 127; C. H. Chang, Y. Q. Chen, Phys. Rev. D46 (1992) 3845; V. V. Kisilev, A. K. Likhoded, M. V. Shevlyagin, preprints IHEP 93-58 and 94-10, Protvino.
- [7] M. Lusignoli, M. Masetti, S. Petrarca, Phys. Lett. B266 (1991) 142.
- [8] E. Brateen, K. Cheung, T. C. Yuan, Phys. Rev. D48 (1993) 4230; R5049; K. Cheung, Phys. Rev. Lett. 71 (1993) 3413.
- [9] K. Kolodziej, A. Leike, R. Rückl, preprint hep-ph 9412249.
- [10] A. V. Berezhnoy, A. K. Likhoded, M. V. Shevlyagin, preprint hep-ph 9408287.
- [11] C. H. Chang, Y. Q. Chen, Phys. Rev. D48 (1993) 4086; C. H. Chang, Y. Q. Chen, G. P. Chang, H. T. Jiang, preprint hep-ph 9408242.
- [12] A. V. Berezhnoy, A. K. Likhoded, M. V. Shevlyagin, preprint hep-ph 9408284.
- [13] S. R. Slabospitsky, preprint hep-ph 94042346.
- [14] H. Stubbe, Comp. Phys. Comm. 8 (1974) 1.
- [15] G. P. Lapage, J. Comp. Phys. 27 (1978) 192.
- [16] A. D. Martin, R. G. Roberts, W. J. Stirling, RAL preprints RAL-94-055 (1994) hep-ph 9406315; RAL-94-104 (1994) hep-ph 9409410; RAL-95-021 (1995) hep-ph 9502336.
- [17] M. Glück, E. Reya, A. Vogt, Z. Phys. C48 (1990) 471; Z. Phys. C53 (1992); Phys. Lett. B306 (1993) 391.

- [18] E. Eichten, I. Hinchliffe, K. Lane, C. Quigg, *Rev. Mod. Phys.* 56 (1984) 579.
- [19] J. Botts et al. *Phys. Lett.* B304 (1993) 159.
- [20] C. A. Dominguez, K. Schilcher, Y. L. Wu, *Phys. Lett.* B298 (1993) 190.
- [21] P. Colangelo, G. Nardulli, M. Pietroni, *Phys. Rev.* D43 (1991) 3002.

Figure Captions

- [1] Feynman diagrams for $g g \rightarrow B_c^+ b \bar{c}$. The complete set of 36 diagram can be obtained from the diagrams shown in the figure performing all possible interchanges of initial gluon momenta and of final quark flavours.
- [2] Total partonic cross section $\hat{\sigma}(g g \rightarrow B_c^+ b \bar{c})$ (in pb).
- [3] Partonic p_T distribution $d\hat{\sigma}/dp_T$ (in pb GeV⁻¹) for $\sqrt{\hat{s}} = 20, 30, 40, 60, 80$ and 100 GeV (in order of increasing p_T endpoint).
- [4] Partonic rapidity distribution $d\hat{\sigma}/dy$ (in pb) for $\sqrt{\hat{s}} = 20, 30, 40, 60, 80$ and 100 GeV (in order of increasing rapidity endpoint).
- [5] Differential cross section $d\sigma/dp_T$ (in nb GeV⁻¹) for direct B_c production calculated with MRS(A) gluon distribution function for LHC ($\sqrt{s} = 14$ TeV) with the evolution scale $Q^2 = 4M_{B_c}^2$ (upper solid line) and $Q^2 = \hat{s}$ (lower solid line), and for Tevatron ($\sqrt{s} = 1.8$ TeV) with the evolution scale $Q^2 = 4M_{B_c}^2$ (upper dotted line) and $Q^2 = \hat{s}$ (lower dotted line).
- [6] Differential cross section $d\sigma/dy_{lab}$ (in nb) for direct B_c production calculated with MRS(A) gluon distribution function for LHC ($\sqrt{s} = 14$ TeV) with the evolution scale $Q^2 = 4M_{B_c}^2$ (upper solid line) and $Q^2 = \hat{s}$ (lower solid line), and for Tevatron ($\sqrt{s} = 1.8$ TeV) with the evolution scale $Q^2 = 4M_{B_c}^2$ (upper dotted line) and $Q^2 = \hat{s}$ (lower dotted line).

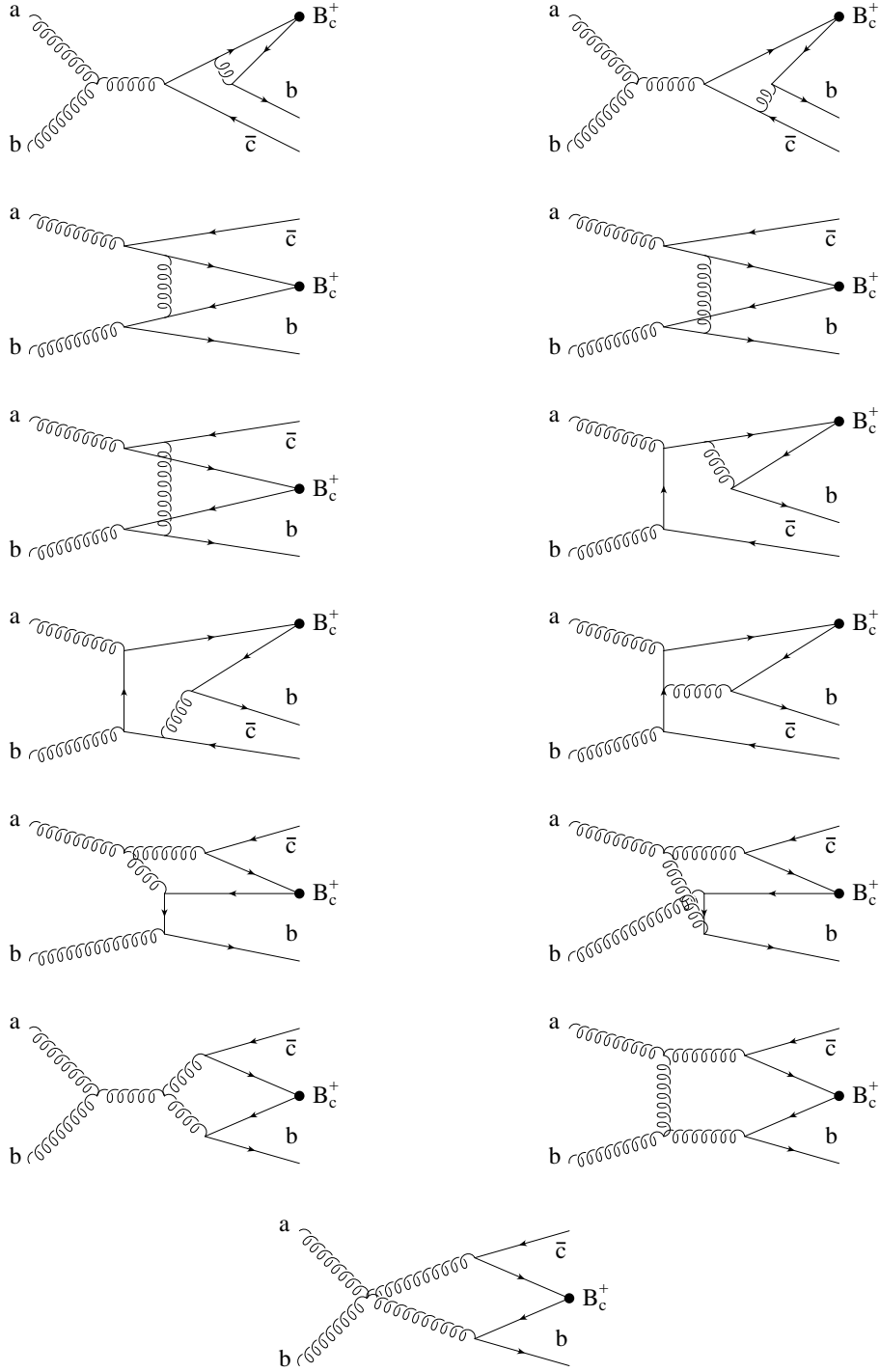


Figure 1:

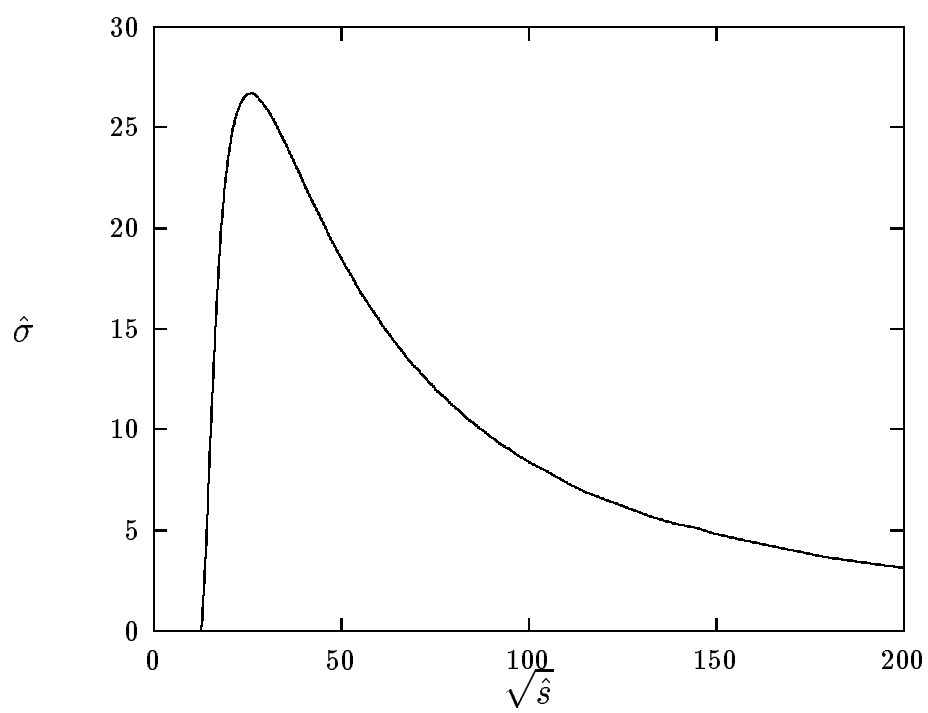


Figure 2:

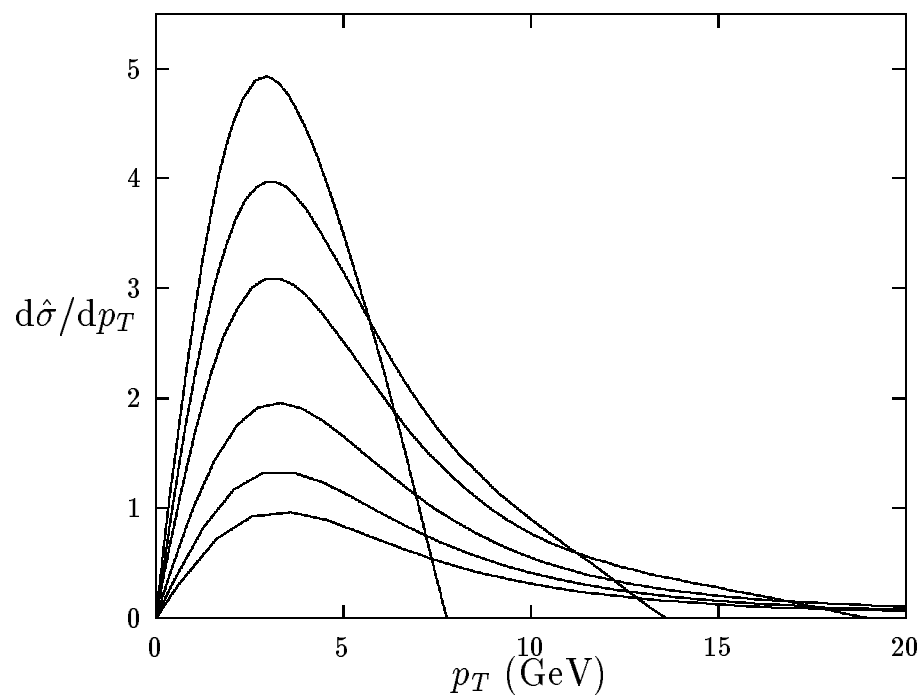


Figure 3:

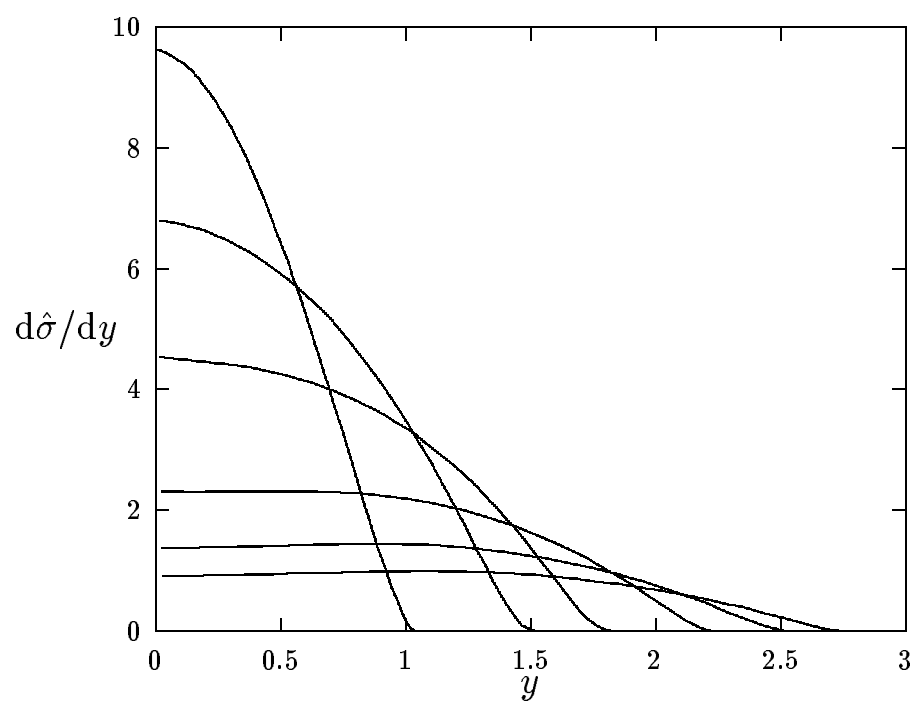


Figure 4:

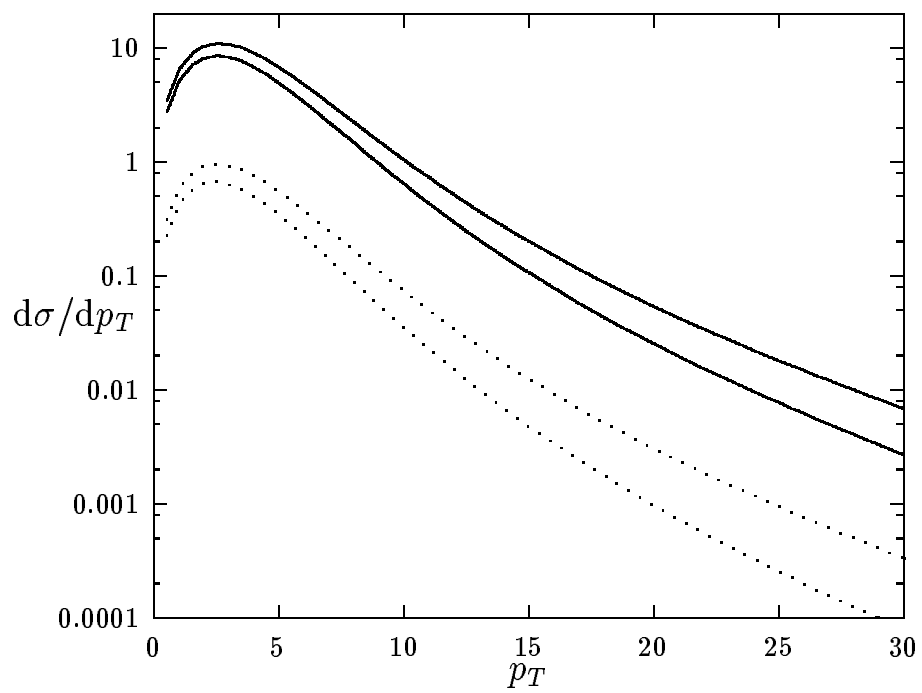


Figure 5:

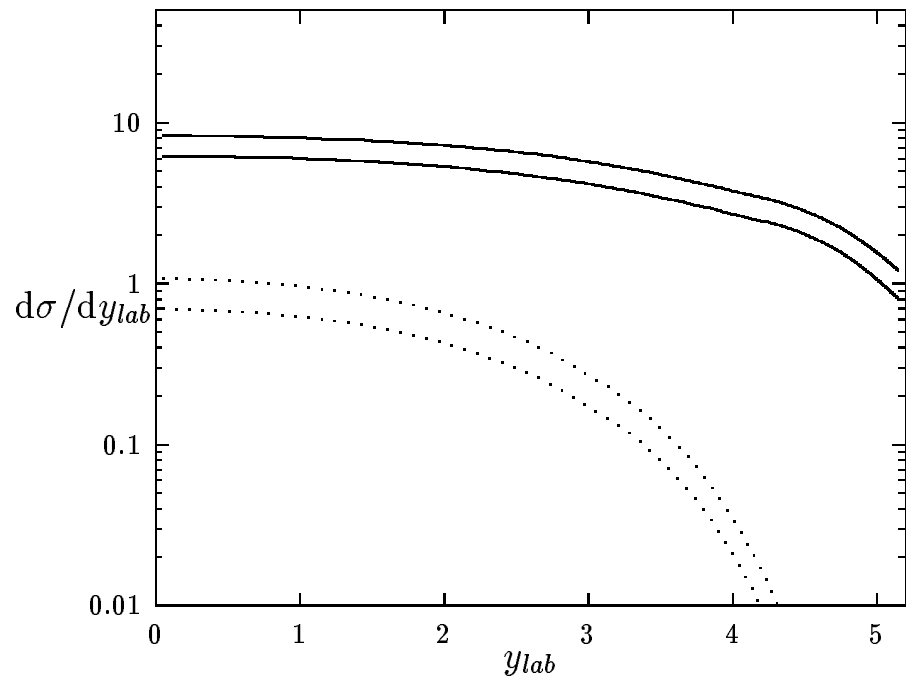


Figure 6: